

Nuclear parton densities and their uncertainties at the next-to-leading order

S. Atashbar Tehrani*

Department of Physics, Yazd Branch, Islamic Azad University, Yazd, Iran and School of Particles and Accelerators,

Institute for Research in Fundamental Sciences (IPM), P.O. Box 19395-5531, Tehran, Iran

(Received 21 October 2012; published 3 December 2012)

Considering the nuclear reactions which involve specific features at certain regions of the x -Bjorken variable which was first observed by the EMC group, we indicate that the parton distributions in nuclei are not simply as the parton densities in nucleons. In addition to the most commonly analyzed data sets for deep-inelastic scattering of charged leptons off nuclei, we also analyze the Drell-Yan dilepton production. We investigate parametrizations of nuclear parton distributions at the next-to-leading order (NLO) of α_s . Finally, optimum nuclear structure functions are determined by a χ^2 analysis of experimental data for the nuclear structure function $F_2^A/F_2^{A'}$ and Drell-Yan cross-section ratios. The related uncertainties are estimated by the Hessian method. Our results are in good agreement with the available experimental data and better than the results of some other fitting parametrization methods.

DOI: 10.1103/PhysRevC.86.064301

PACS number(s): 25.30.Mr, 13.85.Qk, 12.39.-x, 14.65.Bt

I. INTRODUCTION

The nature of the short-distance structure of nucleons is one of the central questions of present day hadron physics. One of the major goals of quantum chromodynamics (QCD) is the particular investigation of the parton distribution of the proton and nuclei, which for the first time has been observed by the European Muon Collaboration (EMC). The important issue in this subject is the different behavior of parton densities in free nucleons and bound nucleons, i.e., nuclei.

Deep inelastic scattering (DIS) experiments which have been performed by NMC, SLAC, NMC, FNAL, BCDMS, HERMES, and JLAB groups [1–16] confirm the specific feature of nuclear reactions at certain regions of the x -Bjorken variable, which was first observed by the EMC. This specific feature has also been seen in Drell-Yan cross-section ratios [17,18]. In this paper we calculate the nuclear parton distribution functions (NPDFs), using the global analysis of experimental data, taking into account the ratio of the structure function, $F_2^A/F_2^{A'}$, and Drell-Yan cross-section ratios $\sigma_{DY}^A/\sigma_{DY}^{A'}$ by employing the QCD PEGASUS package [19].

This paper consists of the following sections. In Sec. II, a formalism to establish an analysis method to parametrize the experimental data is introduced. In Sec. III we do a review on the existed data of the nuclear reactions. Section IV is allocated to the χ^2 analysis. The Hessian method is discussed in Sec. V. We embark from the used analysis to follow our calculations and will yield our results in Sec. VI.

II. FORMALISM

In order to calculate the parton distribution in nuclear media, we need first the parton distributions in a free proton. We then use a PDF set which has been parametrized at the input scale $Q_0^2 = 2 \text{ GeV}^2$ with the following standard form,

quoted from Ref. [20]:

$$\begin{aligned} x u_v(x, Q_0^2) &= A_u x^{\alpha_u} (1-x)^{\beta_u} (1 + \gamma_u x^{\delta_u} + \eta_u x), \\ x d_v(x, Q_0^2) &= A_d x^{\alpha_d} (1-x)^{\beta_d} (1 + \gamma_d x^{\delta_d} + \eta_d x), \\ x s(x, Q_0^2) &= A_s x^{\alpha_s} (1-x)^{\beta_s} (1 + \gamma_s x^{\delta_s} + \eta_s x), \\ x \delta(x, Q_0^2) &= A_\delta x^{\alpha_\delta} (1-x)^{\beta_\delta + \beta_s} (1 + \gamma_\delta x^{\delta_\delta} + \eta_\delta x), \\ x g(x, Q_0^2) &= A_g x^{\alpha_g} (1-x)^{\beta_g} (1 + \gamma_g x^{\delta_g} + \eta_g x). \end{aligned} \quad (1)$$

The PDFs above are used as the valance quark distributions $x u_v$, $x d_v$, the antiquark distributions $x s = \frac{x(\bar{u}+\bar{d}+\bar{s})}{3}$, $x \delta = x(\bar{d}-\bar{u})$, and gluon distribution $x g$. Typical results of using these PDFs to produce F_2 proton structure functions are depicted in Fig. 1. In this figure a comparison between the results of the model used in Ref. [20] and the experimental groups BCDMS, H1, NMC, SLAC, and ZEUS [21–29] has also been done, indicating a good agreement between them. The required relations to provide us the unknown parameters in Eq. (1) are given in Appendix A.

We know the NPDFs are provided by a number of parameters at a fixed Q^2 which are normally denoted by Q_0^2 . The NPDFs are related to PDFs in free protons, and for this purpose nucleonic PDFs are multiplied by a weight function w_i :

$$f_i^A(x, Q_0^2) = w_i(x, A, Z) f_i(x, Q_0^2) \quad (2)$$

The parameters in the weight function are obtained by a χ^2 analysis procedure which is dependent on x , A (mass number), and Z (atomic number).

Here we follow the analysis given by Refs. [30–35] and assume the functional form below for the weight function in Eq. (2):

$$\begin{aligned} w_i(x, A, Z) &= 1 + \left(1 - \frac{1}{A^\alpha}\right) \\ &\times \frac{a_i(A, Z) + b_i(A)x + c_i(A)x^2 + d_i(A)x^3}{(1-x)^{\beta_i}}. \end{aligned} \quad (3)$$

* Atashbar@ipm.ir

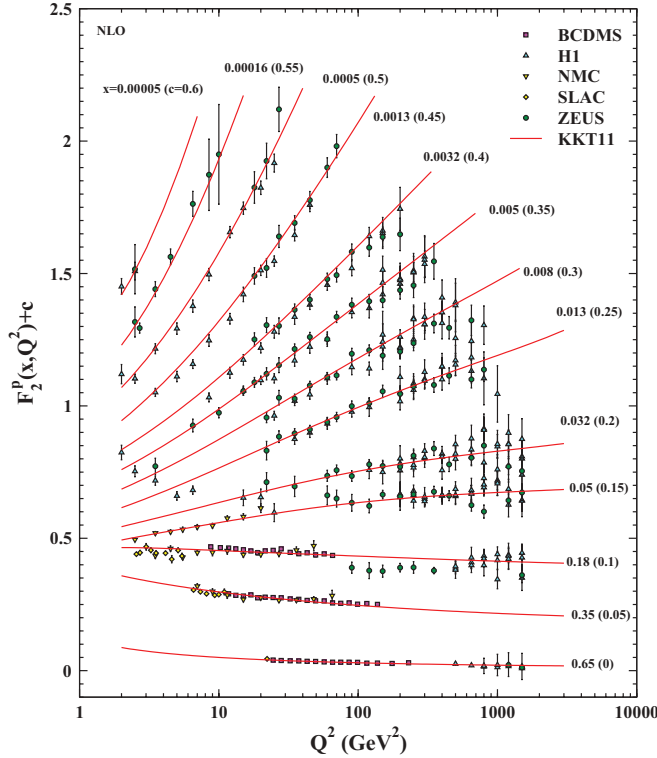


FIG. 1. (Color online) Proton structure function, resulting from the analysis in Ref. [20].

Combining the weight function in Eq. (3) with PDFs in Eq. (2) will yield us us NPDFs as follows:

$$\begin{aligned} u_v^A(x, Q_0^2) &= w_{u_v}(x, A, Z) \frac{Z u_v(x, Q_0^2) + N d_v(x, Q_0^2)}{A}, \\ d_v^A(x, Q_0^2) &= w_{d_v}(x, A, Z) \frac{Z d_v(x, Q_0^2) + N u_v(x, Q_0^2)}{A}, \\ \bar{u}^A(x, Q_0^2) &= w_{\bar{q}}(x, A, Z) \frac{Z \bar{u}(x, Q_0^2) + N \bar{d}(x, Q_0^2)}{A}, \quad (4) \\ \bar{d}^A(x, Q_0^2) &= w_{\bar{q}}(x, A, Z) \frac{Z \bar{d}(x, Q_0^2) + N \bar{u}(x, Q_0^2)}{A}, \\ s^A(x, Q_0^2) &= w_{\bar{q}}(x, A, Z) s(x, Q_0^2), \\ g^A(x, Q_0^2) &= w_g(x, A, Z) g(x, Q_0^2). \end{aligned}$$

In the first four equations, the Z term as atomic number indicates the number of protons and the N ($= A - Z$) term indicates the number of neutrons in the nuclei while the $SU(3)$ symmetry is apparently broken there. If the number of protons and neutrons in a nucleus are equal to each other (isoscalar nuclei) such as in 2D , 4He , ${}^{12}C$, and ${}^{40}Ca$ nuclei, the valence quarks u_v^A and d_v^A and \bar{u}^A and \bar{d}^A would have similar distributions. In the case that Z and A numbers are not equal in the nuclei, it can be concluded that antiquark distributions (\bar{u}^A , \bar{d}^A , \bar{s}^A) in the nuclei would not be equal to each other [36,37]. For the strange quark distributions in the nuclei some research studies are still being done [38], but we assume the common case in which it is assumed $s = \bar{s}$. In Eq. (3) we take $\alpha = 1/3$ as in Ref. [39], considering nuclear

volume and surface contributions. In addition there are three constraints for the parameters in Eq. (3), namely the nuclear charge Z , baryon number (mass number) A , and momentum conservation [30,31,40] as follows:

$$\begin{aligned} Z &= \int \frac{A}{3} [2u_v^A - d_v^A](x, Q_0^2) dx, \\ 3 &= \int [u_v^A + d_v^A](x, Q_0^2) dx, \\ 1 &= \int x[u_v^A + d_v^A + 2\{\bar{u}^A + \bar{d}^A + \bar{s}^A\} + g^A](x, Q_0^2) dx. \end{aligned} \quad (5)$$

III. OVERVIEW OF THE AVAILABLE EXPERIMENTAL DATA

In Table I, we list some of the data prepared by different experimental groups for the F_2^A/F_2^D ratio. In this ratio the numerator denotes the structure function of a nuclei and the

TABLE I. Different experimental results for the F_2^A/F_2^D ratio at $Q^2 \geq 1.0 \text{ GeV}^2$. The number of data points and the related references are also listed.

Nucleus	Experiment	No. of data	Reference
(F_2^A/F_2^D)			
He/D	SLAC-E139	18	[13]
	NMC-95	17	[1]
Li/D	NMC-95	17	[1]
Li/D (Q^2 dep.)	NMC-95	179	[1]
Be/D	SLAC-E139	17	[2]
C/D	EMC-88	9	[8]
	EMC-90	5	[13]
	SLAC-E139	7	[2]
	NMC-95	17	[1]
	FNAL-E665	5	[11]
	JLAB-E03-103	103	[10]
C/D (Q^2 dep.)	NMC-95	191	[1]
N/D	BCDMS-85	9	[14]
	HERMES-03	153	[16]
Al/D	SLAC-E49	18	[3]
	SLAC-E139	17	[2]
Ca/D	EMC-90	5	[13]
	NMC-95	16	[1]
	SLAC-E139	7	[13]
	FNAL-E665	5	[11]
Fe/D	SLAC-E87	14	[4]
	SLAC-E139	23	[2]
	SLAC-E140	10	[5]
	BCDMS-87	10	[6]
Cu/D	EMC-93	19	[7]
Kr/D	HERMES-03	144	[16]
Ag/D	SLAC-E139	7	[2]
Sn/D	EMC-88	8	[8]
Xe/D	FNAL-E665-92	5	[9]
Au/D	SLAC-E139	18	[2]
	SLAC-E140	1	[5]
Pb/D	FNAL-E665-95	5	[11]
F_2^A/F_2^D total			1079

TABLE II. Different experimental results for the $F_2^A/F_2^{A'}$ ratio at $Q^2 \geq 1.0 \text{ GeV}^2$. The number of data points and the related references are also listed.

Nucleus	Experiment	No. of data	Reference
$(F_2^A/F_2^{A'})$			
Be/C	NMC-96	15	[15]
Al/C	NMC-96	15	[15]
Ca/C	NMC-96	24	[1]
	NMC-96	15	[15]
Fe/C	NMC-96	15	[15]
Sn/C	NMC-96	146	[15]
	NMC-96	15	[15]
Pb/C	NMC-96	15	[15]
C/Li	NMC-95	24	[1]
Ca/Li	NMC-95	24	[1]
$F_2^A/F_2^{A'}$ total		308	

denominator represents the structure function of deuterium. The total number of data for the ratio in which the numerator includes nuclei such as helium (He), lithium (Li), etc. is equal to 1079. In Table II the number of $F_2^A/F_2^{A'}$ ratios for Be/C, Al/C, Ca/C, Fe/C, Sn/C, Pb/C, and C/Li is 308. For Drell-Yan cross section ratios in Table III the number of data is equal to 92 while the related ratios are C/D, Ca/D, Fe/D, W/D, Fe/Be, and W/Be. In the employed analysis the total number of data is 1479. The interval range of Q^2 values is $Q^2 \geq 1 \text{ GeV}^2$ and the smallest value for the Bjorken variable x is equal to 0.0055.

IV. ANALYSIS OF THE χ^2 VALUE

We use the MINUIT fitting package [41] to fit the experimental data the structure function $F_2^A/F_2^{A'}$ and Drell-Yan cross-section ratios.

The optimized value of total χ^2 is defined by

$$\chi^2 = \sum_j \frac{(R_j^{\text{data}} - R_j^{\text{theo}})^2}{(\sigma_j^{\text{data}})^2}. \quad (6)$$

This relation yield us the proper parameters for NPDFs. Here R_j^{data} indicates the experimental values for the $F_2^A/F_2^{A'}$ or

TABLE III. Different experimental results for the Drell-Yan cross-section ratios, $\sigma_{DY}^A/\sigma_{DY}^{A'}$, at $Q^2 \geq 1.0 \text{ GeV}^2$. The number of data points and the related references are also listed.

Nucleus	Experiment	No. of data	Reference
$(\sigma_{DY}^A/\sigma_{DY}^{A'})$			
C/D	FNAL-E772-90	9	[18]
Ca/D	FNAL-E772-90	9	[18]
Fe/D	FNAL-E772-90	9	[18]
W/D	FNAL-E772-90	9	[18]
Fe/Be	FNAL-E866/NuSea	28	[17]
W/Be	FNAL-E866/NuSea	28	[17]
$\sigma_{DY}^A/\sigma_{DY}^{A'}$ total		92	

$\sigma_{DY}^A/\sigma_{DY}^{A'}$ ratio and R_j^{theo} denotes the theoretical result for the parameterized NPDFs. In our calculations, we take $Q_0^2 = 2 \text{ GeV}^2$ [20] and the χ^2 analysis is done based on the DGLAP evolution equations [19]. Our calculations are done in the next-to-leading order (NLO) approximation in which the modified minimal subtraction scheme MS is used [42].

Therefore the nuclei structure function is written as follows:

$$F_2^A(x, Q^2) = \sum_{i=u,d,s} e_i^2 x [1 + a_s C_q(x) \otimes] (q_i^A + \bar{q}_i^A)(x, Q^2) + \frac{1}{3} a_s C_g(x) \otimes x g^A(x, Q^2). \quad (7)$$

In this equation, the symbol \otimes denotes the convolution integral:

$$f(x) \otimes g(x) = \int_x^1 \frac{dy}{y} f\left(\frac{x}{y}\right) g(y). \quad (8)$$

We employ the CERN program library MINUIT to minimize the χ^2 value. Following that an error analysis can be done, using the Hessian matrix. The NPDF uncertainties are estimated, using the Hessian matrix as follows:

$$[\delta f^A(x)]^2 = \Delta \chi^2 \sum_{i,j} \left(\frac{\partial f^A(x, \xi)}{\partial \xi_i} \right)_{\xi=\hat{\xi}} \times H_{ij}^{-1} \left(\frac{\partial f^A(x, \xi)}{\partial \xi_j} \right)_{\xi=\hat{\xi}}, \quad (9)$$

where H_{ij} is the Hessian matrix, ξ_i is a quantity referring to the parameters which exist in NPDFs, and $\hat{\xi}$ indicates the amount of the parameter which makes an extremum value for the related derivative. The $\Delta \chi^2$ value determines the confidence region and is given by

$$\Delta \chi^2 \equiv \chi^2(\hat{a} + \delta a) - \chi^2(\hat{a}) = \sum_{i,j} H_{ij} \delta a_i \delta a_j. \quad (10)$$

The $\Delta \chi^2$ value is calculated considering the confidence level P which is defined as

$$P = \int_0^{\Delta \chi^2} \frac{1}{2\Gamma(\frac{N}{2})} \left(\frac{s}{2} \right)^{\frac{N}{2}} \exp\left(-\frac{s}{2}\right) ds. \quad (11)$$

The numerical value of Eq. (11) which corresponds to 1σ error is $P = 0.6826$. This numerical value relates to a given number of parameters (N) by assuming the normal distribution in the multiparameter space. In this equation $\Gamma(m)$ denotes the gamma function. In an analysis with the 16 parameters, we achieve $\Delta \chi^2 = 18.112$. The Hessian method can also be used to estimate the polarized PDFs and fragmentation functions [43].

V. NEIGHBORHOODS AND THE HESSIAN METHOD

We here give just the essential concepts of the Hessian method while the full details can be found in Refs. [43,44]. According to what has been presented in Sec. IV we can find a set of the appropriate parameters which minimize the global χ^2 function. We call this NPDF set S_0 . The numerical values of this set, i.e., p_1^0, \dots, p_n^0 are presenting in Sec. VI. By changing

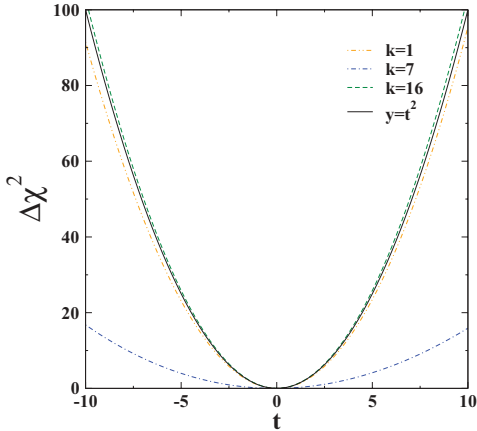


FIG. 2. (Color online) $\Delta\chi^2$ as a function of t defined in Eq. (18) for some random sample eigenvectors.

the parameters from their specified values, χ^2_{global} increases by the amount $\Delta\chi^2_{\text{global}}$ which is defined as

$$\Delta\chi^2_{\text{global}} = \chi^2_{\text{global}} - \chi^2_0 = \sum_{i,j=1}^d H_{ij}(p_i - p_i^0)(p_j - p_j^0), \quad (12)$$

where the Hessian matrix H_{ij} is defined by

$$H_{ij} = \frac{1}{2} \left. \frac{\partial^2 \chi^2_{\text{global}}}{\partial p_i \partial p_j} \right|_{\min} \quad (13)$$

We should note that $C \equiv H^{-1}$ (C denotes the covariant matrix). Now it is convenient to work in term of eigenvalues

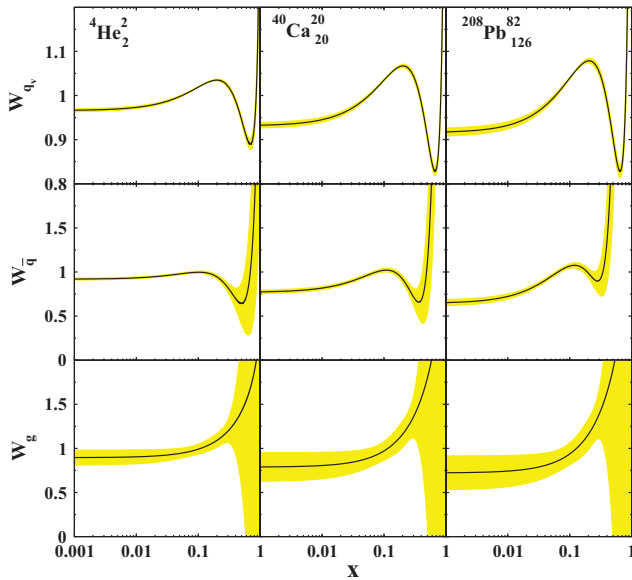


FIG. 3. (Color online) The weight functions for ${}^4\text{He}_2$, ${}^{40}\text{Ca}_{20}$, and ${}^{208}\text{Pb}_{126}$ nuclei at $Q^2 = 2 \text{ GeV}^2$.

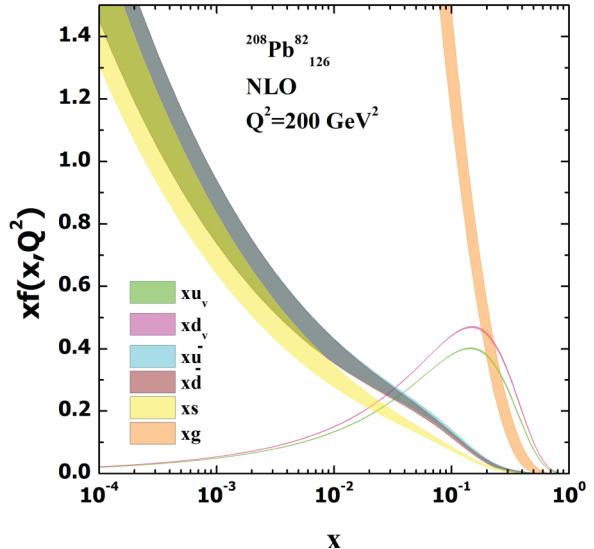


FIG. 4. (Color online) Parton distribution for lead at $Q^2 = 200 \text{ GeV}^2$, including the error band.

and eigenvectors of the covariance matrix

$$\sum_{j=1}^n C_{ij} v_{jk} = \lambda_k v_{ik}, \quad (14)$$

where C_{ij} is i th component of the covariance matrix and λ_k and v_{ik} are the k th eigenvalue and i th component of the k th eigenvector respectively. Also the displacement of parameter p_i from its minimum p_i^0 can be expressed in terms of rescaled eigenvectors $e_{ik} = \sqrt{\lambda_k} v_{ik}$:

$$p_i - p_i^0 = \sum_{k=1}^n e_{ik} z_k. \quad (15)$$

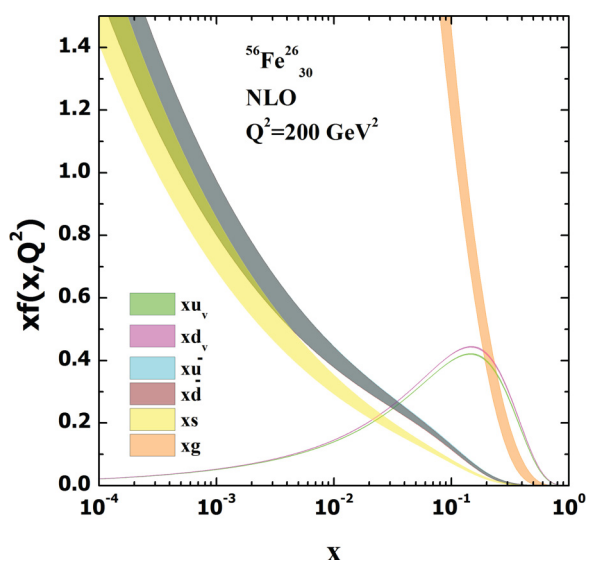


FIG. 5. (Color online) Parton distribution for iron at $Q^2 = 200 \text{ GeV}^2$, including the error band.

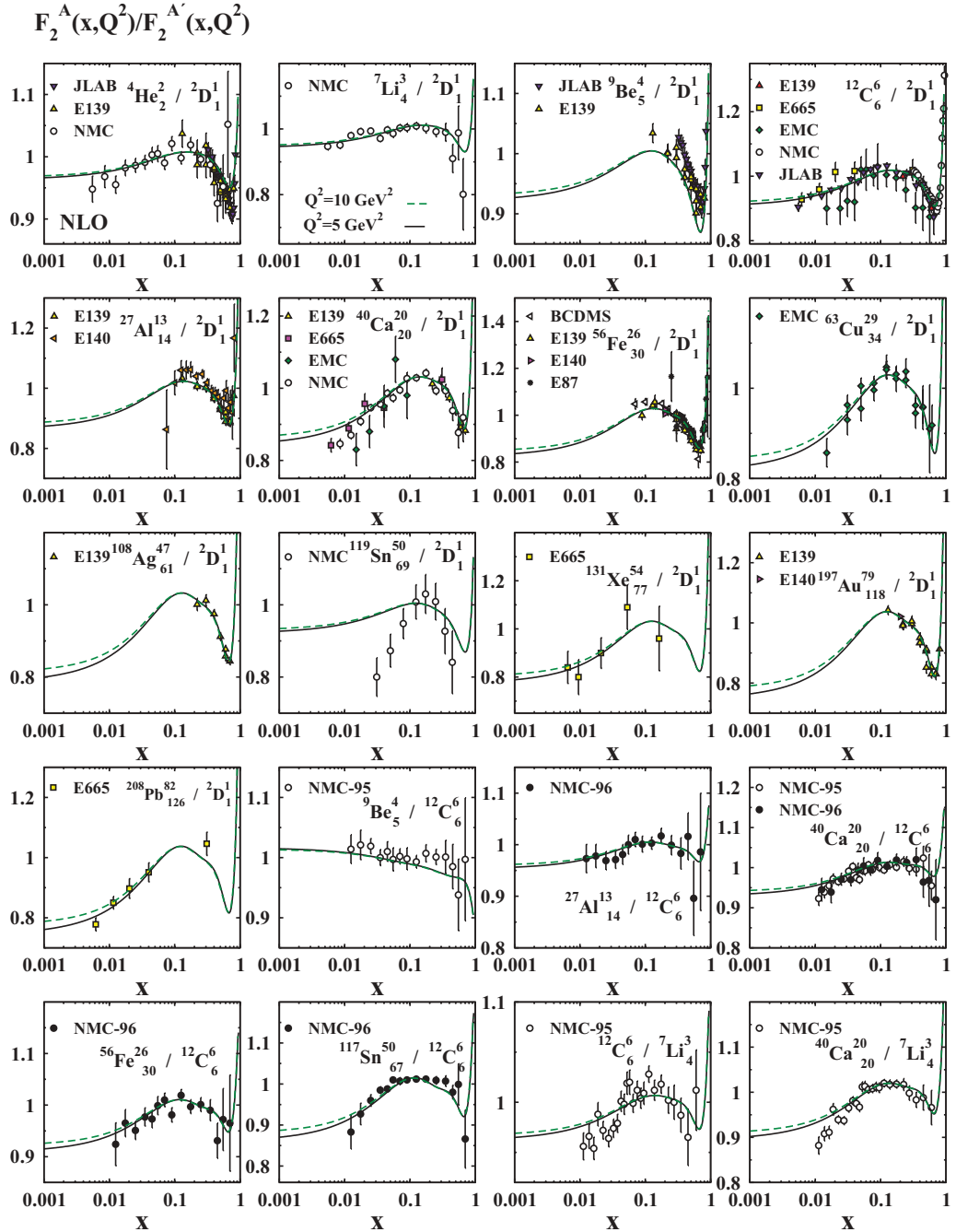


FIG. 6. (Color online) DIS data in nuclear reactions (EMC effects) for $F_2^A/F_2^{A'}$, resulting from our theoretical model at $Q^2 = 5$ and 10 GeV^2 . Comparison with the available date has also been done [1–16].

Replacing Eq. (15) in Eq. (12) and considering the orthogonality of v_k we achieve

$$\Delta\chi_{\text{global}}^2 = \sum_{k=1}^n z_k^n. \quad (16)$$

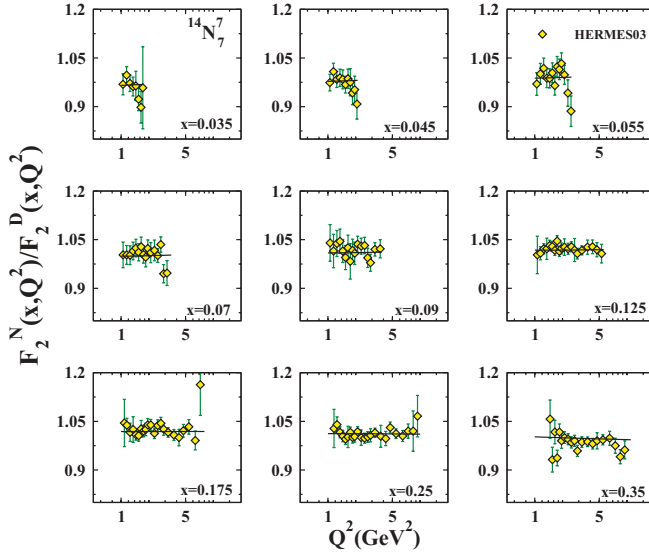
Now the relevant neighborhood of χ_{global}^2 is the interior of a hypersphere with radius T :

$$\sum_{k=1}^n z_k^2 \leq T^2, \quad (17)$$

and the neighborhood parameters are given by

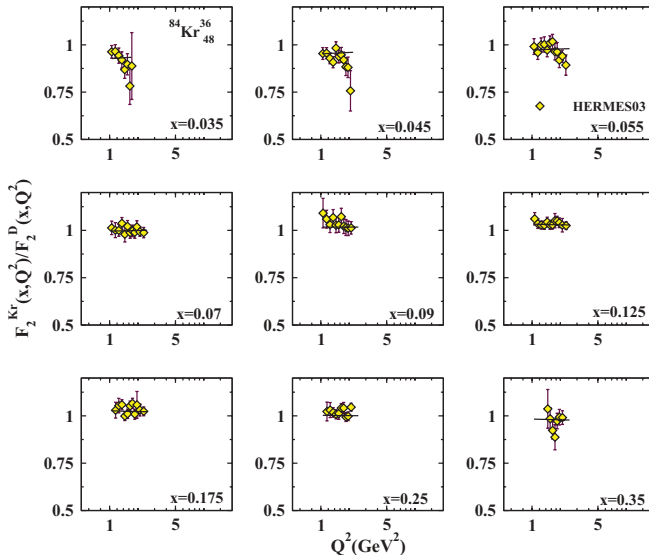
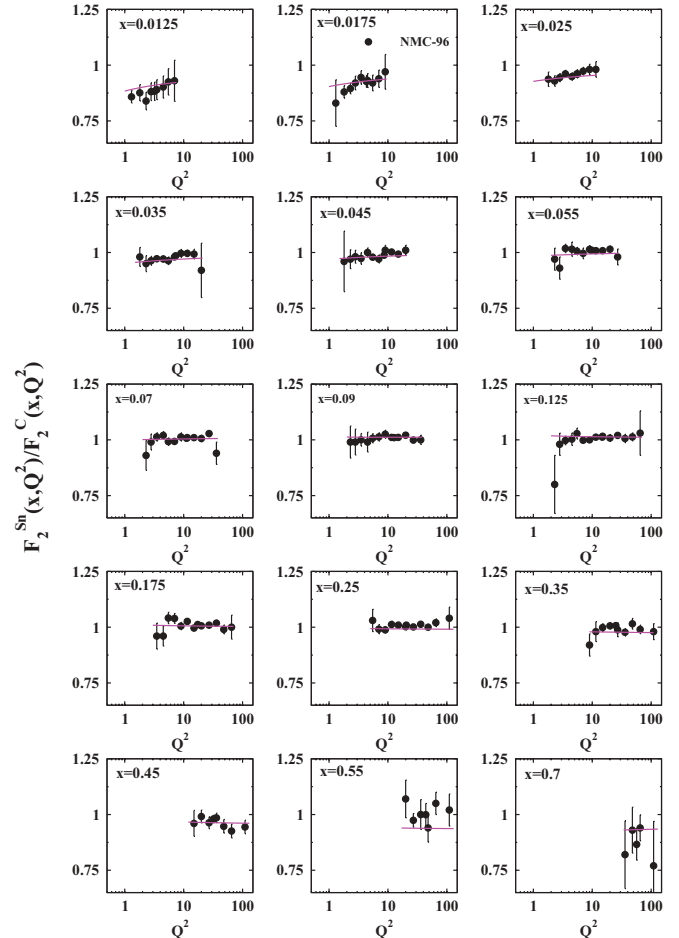
$$p_i(s_k^\pm) = p_i^0 \pm t e_{ik}, \quad (18)$$

where s_k is the k th set of NPDFs and t is adapted to make the desired $T = (\Delta\chi_{\text{global}}^2)^{\frac{1}{2}}$ and $t = T$ in the quadratic approximation. In Fig. 2 we depict the dependance of $\Delta\chi_{\text{global}}^2$ along some random samples of eigenvector directions to test the quadratic approximation of Eq. (12).

FIG. 7. (Color online) Q^2 dependence of F_2^N/F_2^D [16].

VI. RESULTS

In our analysis we use the weight function method as in Ref. [32]. However, in this analysis we assume that the coefficients in Eq. (3) depend on nuclear mass number A . By this assumption we can get to a better value for $\chi^2/\text{D.O.F.}$ with respect to what was done in Ref. [32]. We also use the JLAB experimental data for the F_2^C/F_2^D ratio [10]. In our analysis, which is done in the NLO approximation, we get $\chi^2/\text{D.O.F.} = 1597.94/1463 = 1.092$, which is a 9% improvement with respect to what was done in Ref. [32], and we achieve $\alpha_s(Q^2) = 0.112098$ [20] at the energy scale of the Z -boson mass, $Q^2 = M_z^2$. The number of data points for the nuclei and Drell-Yan ratios totals 1479. The number of parameters used in our fitting procedure is equal to 16. It is worthmentioning that some groups have already worked

FIG. 8. (Color online) Q^2 dependence of F_2^{Kr}/F_2^D [16].FIG. 9. (Color online) Q^2 dependence of F_2^{Sn}/F_2^C [15].

on this subject and provided very elegant FORTRAN codes to analyze the DIS data concerning the nuclear reactions [45–49]. In Fig. 3 we depict the weight functions for the helium, calcium, and lead nuclei at initial value $Q_0^2 = 2 \text{ GeV}^2$. In this figure the uncertainties are indicated by the bands. We extract the PDFs for lead and iron nuclei at $Q^2 = 200 \text{ GeV}^2$ with the related uncertainties for valance quark, sea quark, and gluon distributions and indicate them in Figs. 4 and 5.

We compare in Fig. 6 our theoretical results with the related DIS data. In Figs. 7, 8, and 9 we depict the ratios F_2^N/F_2^D , F_2^{Kr}/F_2^D , and F_2^{Sn}/F_2^C with respect to Q^2 values and compare them with the available experimental data [15,16]. The nuclear parton distribution functions and their uncertainties are determined by analyzing the F_2 and Drell-Yan experimental data. The uncertainties are again estimated by the Hessian method.

We also calculated the calcium and lead parton distributions and compared them with nuclear PDFs resulting from the CTEQ Collaboration (n-CTEQ) [45], HKN-04 [31], and HKN-07 [32] results at $Q^2 = 100 \text{ GeV}^2$ in Figs. 10 and 11. In Fig. 12 we compare the xenon nucleon parton distributions at $Q^2 = 20 \text{ GeV}^2$ with HKN-07 results [32].

Flavor symmetry in nuclei such as ${}^2\text{D}$, ${}^4\text{He}$, ${}^{12}\text{C}$, and ${}^{40}\text{Ca}$ are similar in that $\bar{u} = \bar{d} = s$. For other nuclei such that the

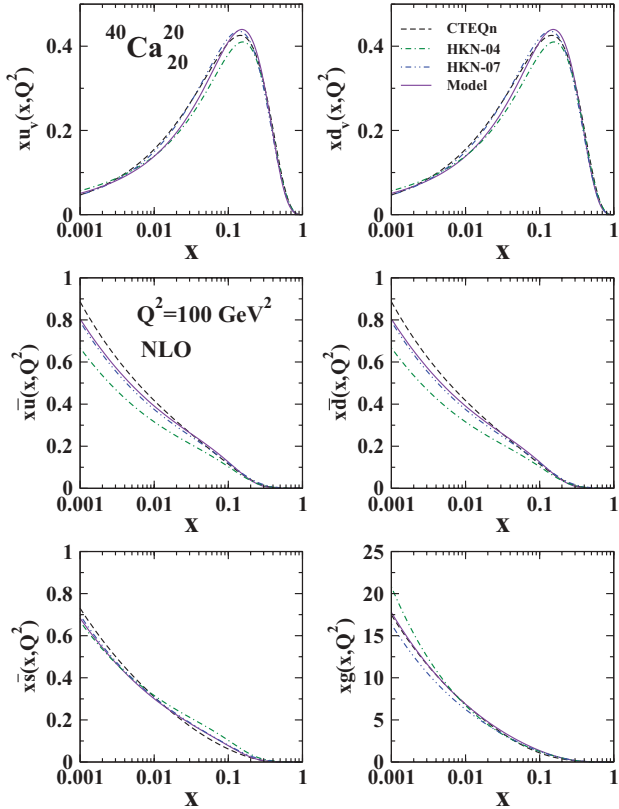


FIG. 10. (Color online) Parton distributions for Calcium at $Q^2 = 100 \text{ GeV}^2$. Comparison with the n-CTEQ [45], HKN-04 [31], and HKN-07 [32] models has also been done.

numbers of their protons and neutrons are not equal, we have the $SU(3)$ flavor symmetry breaking. We compare our model assuming $\bar{u} \neq \bar{d} \neq s$ with HKN-07 [32] and n-CTEQ [45] results. This analysis has been done for gold in Fig. 13 at $Q^2 = 5 \text{ GeV}^2$ in which we have $SU(3)$ symmetry breaking.

If we choose the weight functions to be A dependent, our analysis for the nuclei ratio data would be more precise. Following that, we compare the results of our model at $Q^2 = 5 \text{ GeV}^2$ with the available experimental data for gold and calcium nuclei in Fig. 14. As can be seen, in this case we get better agreement with the already existing experimental data.

Our analysis have been done in two steps. In the first step 19 parameters have been optimized by minimizing the χ^2 value, and in the second one since we fixed three parameters β_v , $\beta_{\bar{q}^A}$, and β_g we just need to determine 16 parameters of the weight functions via our fitting procedure. The reason that we have to fix these three parameters is to control the Fermi motions of the partons inside the nuclei at small values of x . For the weight functions of the valance and sea quark distributions, we choose an A -dependent function while the weight function for the gluon distribution is assumed independent of A number. The numerical values in Table IV, are listed on this basis. The parameters a_{u_v} , a_{d_v} , and a_g are fixed by the three sum rules given in Eq. (6).

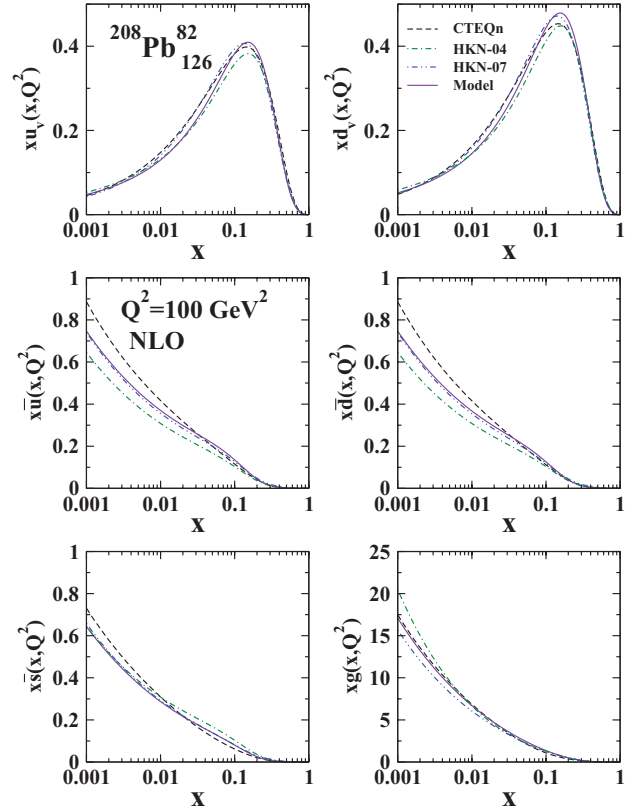


FIG. 11. (Color online) Parton distributions for lead with $Q^2 = 100 \text{ GeV}^2$ and comparison with the n-CTEQ [45], HKN-04 [31], and HKN-07 [32] results.

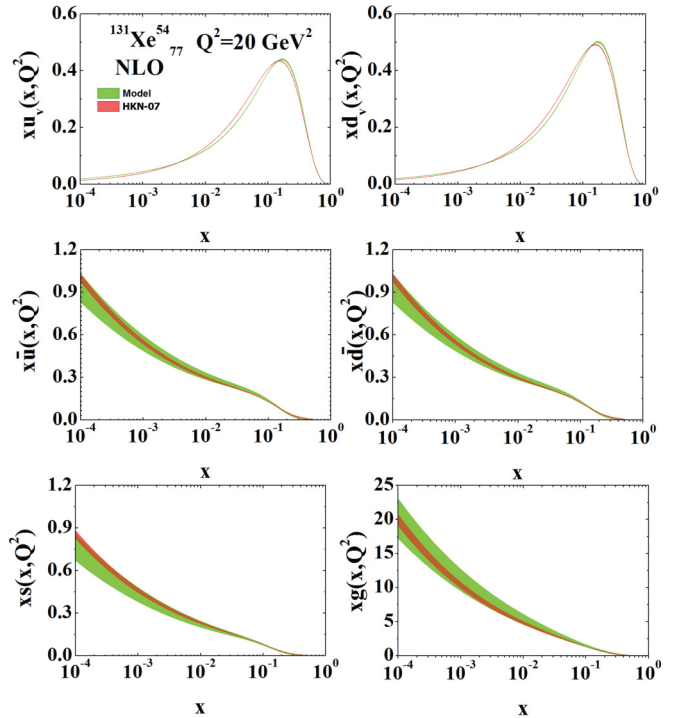


FIG. 12. (Color online) Parton distributions in xenon at $Q^2 = 20 \text{ GeV}^2$ and comparison with HKN-07 [32] results, including error band.

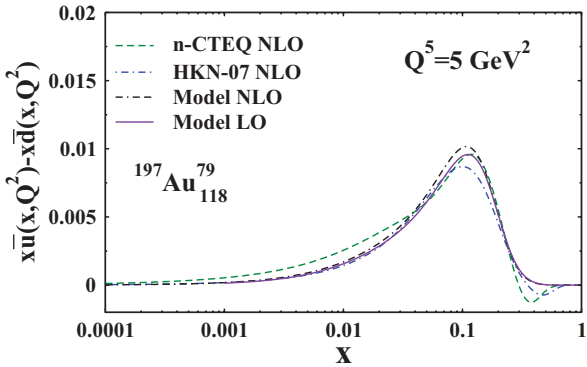


FIG. 13. (Color online) Flavor symmetry $x\bar{u} - x\bar{d}$ in gold at $Q^2 = 5 \text{ GeV}^2$ and comparison with HKN-07 [32] and n-CTEQ [45] results.

ACKNOWLEDGMENTS

S.A.T. is grateful to Ami Rostomyan from the HERMES management group, John R. Arrington from the JLAB group, and Marco Stratmann from Brookhaven National Laboratory for providing the DIS experimental data which were used in the analysis. The author is also indebted to M. Hirai and S. Kumano for giving the required grid data, and thanks them for reading the manuscript and giving useful comments. F. Olness from SMU is specially acknowledged for reading the paper and giving crucial comments. The author is also thankful to the Yazd Branch, Islamic Azad University, for supporting him financially for this project.

APPENDIX A

Having three sum rules which give us the nuclear charge Z , baryon number A , and momentum conservation as in Eq. (6), we can calculate the three parameters $a_{u_v}(A, Z)$, $a_{d_v}(A, Z)$, and $a_g(A, Z)$:

$$a_{u_v}(A, Z) = -\frac{ZI_1(A) + (A - z)I_2(A)}{ZI_3 + (A - Z)I_4},$$

$$a_{d_v}(A, Z) = -\frac{ZI_2(A) + (A - z)I_1(A)}{ZI_4 + (A - Z)I_3},$$

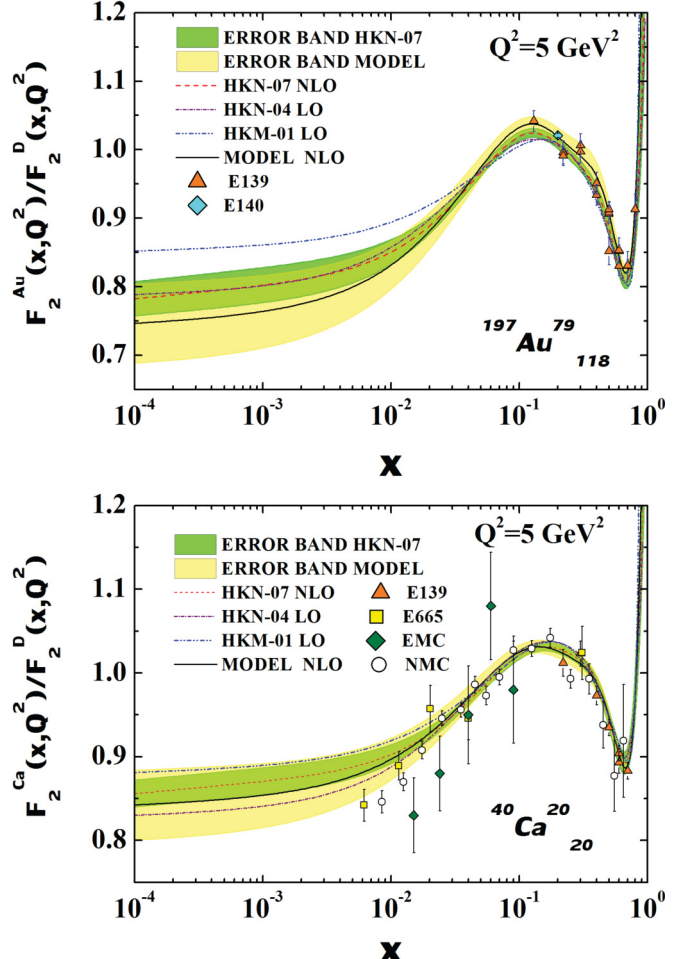


FIG. 14. (Color online) DIS data in nuclear reactions (EMC effect) for gold and calcium at $Q^2 = 5 \text{ GeV}^2$ and comparison with the results from HKN-01 [30], HKN-04 [31], and HKN-07 [32].

$$a_g(A, Z) = -\frac{1}{I_8} \left\{ a_{u_v}(A, Z) \left[\frac{Z}{A} I_5 + \left(1 - \frac{Z}{A} \right) I_6 \right] + a_{d_v}(A, Z) \left[\frac{Z}{A} I_6 + \left(1 - \frac{Z}{A} I_5 \right) \right] + I_7(A) \right\}. \quad (\text{A1})$$

TABLE IV. Parameters obtained by analyzing the weight functions for valance quark, sea quark, and gluon distributions.

a_v	u_v^A and d_v^A distributions					β_v
	b_v	c_v	d_v	β_v		
Appendix A	$2.019A^{8.25 \times 10^{-3}}$	$-6.749A^{6.135 \times 10^{-3}}$	$5.18A^{1.49 \times 10^{-2}}$	0.4		
$a_{\bar{q}^A}$	$b_{\bar{q}^A}$	$c_{\bar{q}^A}$	$d_{\bar{q}^A}$	$\beta_{\bar{q}^A}$		
$-0.177A^{0.166 \times 10^{-2}}$	$3.369A^{0.206}$	$-19.75A^{0.21}$	$19.12A^{0.311}$	0.1		
a_g	b_g	c_g	d_g	β_g		
Appendix A	2.596	0.369	0.369	0.1		

To obtain the numerical values for these parameters in any nuclei, we need to calculate the following integrals [32]:

$$\begin{aligned} I_1(A) &= \int \frac{H_v(x, A)}{(1-x)^{\beta_v}} u_v(x) dx, \quad I_2(A) = \int \frac{H_v(x, A)}{(1-x)^{\beta_v}} d_v(x) dx, \\ I_3 &= \int \frac{1}{(1-x)^{\beta_v}} u_v(x) dx, \quad I_4 = \int \frac{1}{(1-x)^{\beta_v}} d_v(x) dx, \\ I_5 &= \int \frac{x}{(1-x)^{\beta_v}} u_v(x) dx, \quad I_6 = \int \frac{x}{(1-x)^{\beta_v}} d_v(x) dx, \\ I_7(A) &= \int x \left[\frac{H_v(x, A)}{(1-x)^{\beta_v}} \{u_v(x) + d_v(x)\} \right. \\ &\quad \left. + \frac{a_{\bar{q}}(A) + H_{\bar{q}}(x, A)}{(1-x)^{\beta_{\bar{q}}}} 2\{\bar{u}(x) + \bar{d}(x) + \bar{s}(x)\} \right. \\ &\quad \left. + \frac{H_g(x, A)}{(1-x)^{\beta_g}} g(x) \right] dx, \\ I_8 &= \int \frac{x}{(1-x)^{\beta_g}} g(x) dx, \end{aligned} \quad (\text{A2})$$

where $\beta_v = 0.4$, $\beta_{\bar{q}} = \beta_g = 0.1$, and $H_i(x, A)$ is given by

$$\begin{aligned} H_v(x, A) &= b_v(A)x + c_v(A)x^2 + d_v(A)x^3, \\ H_{\bar{q}}(x, A) &= b_{\bar{q}}(A)x + c_{\bar{q}}(A)x^2 + d_{\bar{q}}(A)x^3, \\ H_g(x) &= b_g + d_g x^3 dx. \end{aligned} \quad (\text{A3})$$

The results of the eight integrals in above depend on the atomic number and are different for each nuclei.

APPENDIX B

The FORTRAN package containing our unpolarized structure functions $F_2^A(x, Q^2)$ for nuclei, as well as the unpolarized parton densities $xu_v^A(x, Q^2)$, $xd_v^A(x, Q^2)$, $xs^A(x, Q^2)$, $x\bar{u}^A(x, Q^2)$, $x\bar{d}^A(x, Q^2)$, $xg^A(x, Q^2)$ and their uncertainties at NLO approximation in the $\overline{\text{MS}}$ scheme can be found at [<http://particles.ipm.ir/links/QCD.htm>] or can be obtained via e-mail from the author. In this package we assumed $10^{-4} \leq x \leq 0.999$ and $1 \leq Q^2 \leq 10^5 \text{ GeV}^2$.

-
- [1] P. Amaudruz *et al.* (New Muon Collaboration), *Nucl. Phys. B* **441**, 3 (1995).
- [2] J. Gomez, R. G. Arnold, P. E. Bosted, C. C. Chang, A. T. Katramatou, G. G. Petratos, A. A. Rahbar, S. E. Rock *et al.*, *Phys. Rev. D* **49**, 4348 (1994).
- [3] A. Bodek, N. Giokaris, W. B. Atwood, D. H. Coward, D. L. Dubin, M. Breidenbach, J. E. Elias, J. I. Friedman *et al.*, *Phys. Rev. Lett.* **51**, 534 (1983).
- [4] A. Bodek, N. Giokaris, W. B. Atwood, D. H. Coward, D. Sherden, D. L. Dubin, J. E. Elias, J. I. Friedman *et al.*, *Phys. Rev. Lett.* **50**, 1431 (1983).
- [5] S. Dasu, P. de Barbaro, A. Bodek, H. Harada, M. W. Krasny, K. Lang, E. M. Riordan, R. Arnold *et al.*, *Phys. Rev. Lett.* **60**, 2591 (1988).
- [6] A. C. Benvenuti *et al.* (BCDMS Collaboration), *Phys. Lett. B* **189**, 483 (1987).
- [7] J. Ashman *et al.* (European Muon Collaboration), *Z. Phys. C* **57**, 211 (1993).
- [8] J. Ashman *et al.* (European Muon Collaboration), *Phys. Lett. B* **202**, 603 (1988).
- [9] M. R. Adams *et al.* (E665 Collaboration), *Phys. Rev. Lett.* **68**, 3266 (1992).
- [10] J. Seely, A. Daniel, D. Gaskell, J. Arrington, N. Fomin, P. Solvignon, R. Asaturyan, F. Benmokhtar *et al.*, *Phys. Rev. Lett.* **103**, 202301 (2009).
- [11] M. R. Adams *et al.* (E665 Collaboration), *Z. Phys. C* **67**, 403 (1995).
- [12] M. Arneodo *et al.* (New Muon. Collaboration), *Nucl. Phys. B* **441**, 12 (1995).
- [13] M. Arneodo *et al.* (European Muon Collaboration), *Nucl. Phys. B* **333**, 1 (1990).
- [14] G. Bari *et al.* (BCDMS Collaboration), *Phys. Lett. B* **163**, 282 (1985).
- [15] M. Arneodo *et al.* (New Muon Collaboration), *Nucl. Phys. B* **481**, 3 (1996).
- [16] K. Ackerstaff *et al.* (HERMES Collaboration), *Phys. Lett. B* **475**, 386 (2000); **567**, 339(E) (2003).
- [17] M. A. Vasiliev, M. E. Beddo, C. N. Brown, T. A. Carey, T. H. Chang, W. E. Cooper, C. A. Gagliardi, G. T. Garvey, D. F. Geesaman, E. A. Hawker, X. C. He, L. D. Eisenhower, D. M. Kaplan, S. B. Kaufman, D. D. Koetke, W. M. Lee, M. J. Leitch, P. L. McGaughey, J. M. Moss, B. A. Mueller, V. Papavassiliou, J. C. Peng, G. Petitt, P. E. Reimer, M. E. Sadler, W. E. Sondheim, P. W. Stankus, R. S. Towell, R. E. Tribble, J. C. Webb, J. L. Willis, and G. R. Young, *Phys. Rev. Lett.* **83**, 2304 (1999).
- [18] D. M. Alde, H. W. Baer, T. A. Carey, G. T. Garvey, A. Klein, C. Lee, M. J. Leitch, J. W. Lillberg *et al.*, *Phys. Rev. Lett.* **64**, 2479 (1990).
- [19] A. Vogt, *Comput. Phys. Commun.* **170**, 65 (2005).
- [20] H. Khanpour, Ali N. Khorramia, and S. Atashbar Tehrani, *Few-Body Syst.* **52**, 279 (2012).
- [21] C. Adloff *et al.* (H1 Collaboration), *Eur. Phys. J. C* **13**, 609 (2000).
- [22] C. Adloff *et al.* (H1 Collaboration), *Eur. Phys. J. C* **19**, 269 (2001).
- [23] C. Adloff *et al.* (H1 Collaboration), *Eur. Phys. J. C* **21**, 33 (2001).
- [24] C. Adloff *et al.* (H1 Collaboration), *Eur. Phys. J. C* **30**, 1 (2003).
- [25] J. Breitweg *et al.* (ZEUS Collaboration), *Eur. Phys. J. C* **7**, 609 (1999).
- [26] S. Chekanov *et al.* (ZEUS Collaboration), *Eur. Phys. J. C* **21**, 443 (2001).
- [27] M. Arneodo *et al.* (New Muon Collaboration), *Nucl. Phys. B* **483**, 3 (1997).
- [28] A. C. Benvenuti *et al.* (BCDMS Collaboration), *Phys. Lett. B* **223**, 485 (1989).
- [29] M. R. Adams *et al.* (E665 Collaboration), *Phys. Rev. D* **54**, 3006 (1996).
- [30] M. Hirai, S. Kumano, and M. Miyama, *Phys. Rev. D* **64**, 034003 (2001).
- [31] M. Hirai, S. Kumano, and T.-H. Nagai, *Phys. Rev. C* **70**, 044905 (2004).
- [32] M. Hirai, S. Kumano, and T.-H. Nagai, *Phys. Rev. C* **76**, 065207 (2007).

- [33] S. A. Tehrani, A. N. Khorramian, and A. Mirjalili, *Int. J. Mod. Phys. A* **20**, 1927 (2005).
- [34] S. A. Tehrani, A. Mirjalili, and A. N. Khorramian, *Nucl. Phys. Proc. Suppl.* **164**, 30 (2007).
- [35] S. A. Tehrani and A. N. Khorramian, in *MENU 2007: 11th International Conference on Meson-Nucleon Physics and the Structure of the Nucleon*, IKP, Forschungszentrum Jülich, Germany, 2007, edited by H. Machner and S. Krewald, SLAC eConf C070910 (SLAC, Stanford, 2007).
- [36] S. Kumano, *Phys. Rep.* **303**, 183 (1998).
- [37] G. T. Garvey and J.-C. Peng, *Prog. Part. Nucl. Phys.* **47**, 203 (2001).
- [38] A. Kusina, T. Stavreva, S. Berge, F. I. Olness, I. Schienbein, K. Kovarik, T. Jezo, J. Y. Yu *et al.*, *Phys. Rev. D* **85**, 094028 (2012).
- [39] I. Sick and D. Day, *Phys. Lett. B* **274**, 16 (1992).
- [40] L. L. Frankfurt, M. I. Strikman, and S. Liuti, *Phys. Rev. Lett.* **65**, 1725 (1990).
- [41] F. James, CERN Program Library Long Writeup D506, 1994 (unpublished).
- [42] M. Gluck, E. Reya, and A. Vogt, *Z. Phys. C* **48**, 471 (1990).
- [43] J. Pumplin, D. Stump, R. Brock, D. Casey, J. Huston, J. Kalk, H. L. Lai, and W. K. Tung, *Phys. Rev. D* **65**, 014013 (2001); *J. High Energy Phys.* 07 (2002) 012; A. D. Martin *et al.*, *Eur. Phys. J. C* **28**, 455 (2003); **35**, 325 (2004).
- [44] A. D. Martin, W. J. Stirling, R. S. Thorne, and G. Watt, *Eur. Phys. J. C* **63**, 189 (2009).
- [45] I. Schienbein, J. Y. Yu, K. Kovarik, C. Keppel, J. G. Morfin, F. I. Olness, and J. F. Owens, *Phys. Rev. D* **80**, 094004 (2009).
- [46] K. J. Eskola, V. J. Kolhinen, and C. A. Salgado, *Eur. Phys. J. C* **9**, 61 (1999).
- [47] K. J. Eskola, V. J. Kolhinen, and P. V. Ruuskanen, *Nucl. Phys. B* **535**, 351 (1998).
- [48] D. de Florian and R. Sassot, *Phys. Rev. D* **69**, 074028 (2004).
- [49] L. Frankfurt, V. Guzey, and M. Strikman, *Phys. Rep.* **512**, 255 (2012).